

An Investigation of the Journal Bearing Friction at the Dynamically Loaded Micro-Grooved and Non-Grooved Bearings

Hakan Adatepe*

Giresun University, Faculty of Engineering,
Department of Energy Systems Engineering

Abstract:- In this study, performances of engine bearings with microgrooved circumferentially, transversally and as herringbone (V-shaped) on their surfaces were investigated under dynamic loading conditions both experimentally and numerically. The frictional force resulted from the applied dynamic load on the bearings was determined experimentally by using a developed frictional force measuring device. Finally, the results of performances of the microgrooved bearings and those of plain bearings were compared and presented.

Keywords : Engine bearings, microgrooved bearings, dynamic load, frictional force

1. INTRODUCTION

It is extremely important for journal bearing designers to predetermine frictional performances of the bearings used for shaft housing applications like in internal combustion engines, jet engines, compressors, piston pumps, mechanical presses, rolling mills and a number of machines. A new generation of bearings with micro grooves which is recently, found in literatures is now be used particularly in automotive engines operating at extreme conditions. In most of the bearings encountered in literature, the bearing surfaces are assumed to be plain (smooth). There are only few studies in the literature on bearings with rough surfaces or the ones with microgrooved surfaces. The reason for this is the difficulties in producing bearing surfaces under strict control and failure of the supporting experiments to the theories put forward on this topic [1]. Zhang and Qiu [2], conducted a theoretical investigation on effects of geometric structure of journal bearing surfaces under dynamic loading and hydrodynamic lubrication conditions. Here, the researchers investigated the effects of surfaces roughness of dynamically loaded finite journal bearings on longitudinal, transversal and isotropic (thoroughly) basis. In their analysis, they used a statistical method (Stochastic Model) that is based on estimation principles developed by Christensen [3,4]. They found that the maximum oil film pressure on a bearing that is accepted to be transversely rough is higher than those of longitudinal and isotropic rough conditions. The researchers also concluded that oil film thickness for an isotropic rough condition is less than those of transversal and longitudinal rough bearings. In a study conducted by Hargreaves ve Armatys [5], performances of three types of microgrooved (transverse and longitudinal grooves made on plain bearing surfaces) journal bearings under different static and dynamic load were investigated. A sample of bearing dynamic load in a near sinusoidal form and on a single axis was applied on a bearing by using a cam mechanism. Variations of frictional moments within liquid friction zone under different static loads suspended on the bearing and at operating speeds of 400-2000 rpm were determined. The researchers found that at high operating speeds bearings with circumferential grooves possess lower frictional moments as compared to the other types. Hata, Nakahara and Aoki investigated the effects of frictional characteristics on surface roughness under mixed and hydrodynamic lubrication conditions by using a test device that operates on pin-disc principles. The roughness on bearing surface was cut precisely in a triangular and trapezoidal shape. It was found that the friction on transversally grooved surface is higher than the friction on plain and longitudinally grooved bearing surfaces [6]. Nakahara remarked that it is extremely difficult to achieve accurate measurements for surface roughness on hydrodynamic lubrication characteristics. This is related to the difficulties in measuring film layer thicknesses among rough surfaces [7]. Nakahara, Takesue and Aoki achieved to measure effects of surface roughness on friction characteristics after cutting regular and irregular threads on rectangular specimens spinning on a small axis and used a test device that operates on pin-disc principles. They found that the results they obtained from this experiment correlated with both theoretical and experimental results. The researchers came to conclude that the effects of roughness on transverse rough surface are greater than those on the longitudinal rough surface [8]. In order to meet today's needs, Watanabe et al developed high performance microgrooved engine bearings by cutting circumferential grooves on plain journal bearings. They also conducted an experimental study, recently, on microgrooved journal bearings. In their study, the researchers determined bearing performances of the microgrooved bearings by applying hydrodynamic and elastohydrodynamic lubrication theory. According to recent studies conducted in Japan on performances of microgrooved bearings it has been, theoretically, shown that circumferentially micro grooves (on bearings) enhances dynamic characteristics of the bearings. Moreover; it was also shown that circumferentially grooved bearings are stronger in terms of resistance against deformation and wear as compared to straight journal bearings. As the oil flow rate increases, the bearing temperature in the grooved bearings becomes less than that of the bearings without microgrooved and as the oil remains in the grooves, the possibility for the bearings to fade is low [9,10,11]. Effects of microgrooves on have direct impacts on journal bearings operating under dynamic loading conditions. That is why it is very important, on the basis of design, to predetermine the behavior of the microgrooves particularly their frictional behavior.

Effect of surface texturing on hydrodynamic performance of journal bearings research paper was about the effect of different surface texture if introduced on the inner surface of the bearing regarding their performance with and without the surface texture. There are two examples of texturing i.e. partial and full texturing. Tonder was the first to mention the partial texturing he found that putting series of dimples or roughness increases the load carrying capacity and more oil film pressure. Carrying out many numerical investigation and combination of textures and considering different parameters all studies conclude that it has positive effect on the performance of the bearing but choosing the texture is important on this basis of the application of bearing. Also a comparative study has been carried out between the partially textured bearing and plain bearing using parameters such as textured length and depth, load carrying capacity and oil film pressure distribution at eccentricity ratio 0.1, 0.2. From the numerical solution it was found that the load carrying capacity and a significant improvement achieved for oil film pressure at $n = 0.1$ and $n = 0.2$ considering two textured angle length $\Theta_g = 30$ and $\Theta_g = 60$. In our study circumferential, transversal and V-shaped grooves were cut on plain surfaces of engine journal bearings. The frictional behavior of the microgrooved bearings and that of the plain bearings under dynamic load were investigated both experimentally and numerically. Then their results were presented. In this study, ORBIT advanced analysis program developed by Ricardo Company for analyzing dynamically loaded journal bearings was used [12]. With this program which the best among computer aided analysis programs for journal bearings, solutions were executed by using mobility method and finite difference method. Moreover; an additional program which operates on Schaffrath method was prepared with which the bearings frictional behavior was numerically presented. [12,13,14,15].

2. NUMERICAL BACKGROUND

The mobility method (References 1 and 2) is a technique used extensively in the automotive industry since its inception approximately 50 years ago. It provides a solution extremely rapidly, typically taking only seconds or a few minutes of CPU time for a typical model, since it does not involve solving the Reynolds Equation. The limitation is that it may be used only in cases of ideal circular bearings without oil feed holes or grooves. However, it does provide a quick initial estimate of operating clearances for any design project related to journal bearings.

In the mobility method, the effect of rotation is converted to an equivalent squeeze motion under steady load. The mobility vector (M), which is the dimensionless squeeze velocity with which a non-rotating shaft moves to support the load, is then calculated. The squeeze velocity (ϵ') for a rotating shaft can then be expressed as

$$\epsilon' = \frac{|F| [C/R]^2}{L D \eta / C} M + \omega \cdot e \quad (1)$$

where; F is bearing load, C radial clearance, R bearing radius, L bearing length, D bearing diameter, η lubricant viscosity, M mobility vector, e eccentricity and ω is bearing rotational speed.

In dynamic analyses, the components of mobility vector (M) can be obtained in two ways. In the first way, the components can be determined instantaneously through mobility maps; whereas, in the second way, the components are calculated by making use of an analytic curve similarity method, as it is done in the ORBIT program [10]. Generally; the mobility vector is expressed as given below:

$$M = f(\epsilon, \gamma) \quad (2)$$

Here; ϵ is the eccentricity ratio (e/C) and γ is the bearing's width to diameter ratio (B/D).

The analytical equations for mobility components by curve similarity method as used in journal bearings analyses are in the following manners:

$$M_x = \frac{f(\alpha, \gamma)}{\pi \gamma^2} \left\{ \sqrt{3\pi} - 0.24\gamma^2 e + \frac{\beta^2}{1-\alpha} (1 - 0.4\sqrt{1-\alpha}) + \alpha^2 \gamma (4/3 - \gamma) \right\} \quad (3)$$

$$M_y = \frac{-\beta}{(1-\alpha)} f(\alpha, \gamma) \left\{ \begin{array}{l} \frac{5}{4} + \frac{\alpha\gamma}{7} + \frac{\alpha^2}{8} (1+\alpha) - 0.3\gamma^2 \left(1 + \frac{\alpha^3}{2\sqrt{3}} \right) + \frac{2\beta^2}{15(1-\alpha)} \\ -0.016 \left(1 - \frac{0.034}{\gamma^2} \right) \frac{1}{(1.03-\alpha)} \end{array} \right\} \quad (4)$$

$$f(\alpha, \gamma) = \frac{(1-\alpha)^2}{\pi \gamma^2} \left[1 + \frac{\gamma^2}{2(1-\alpha)} \right] \quad (5)$$

Here; α and β are the eccentricity ratios in X and Y directions respectively.

The second method provided by this commercial software is based on a direct finite difference solution of the Reynolds equation [13]:

with the following boundary conditions:

The Schaffrath method [14,15] is the last computational program used in this study to test performances of dynamically loaded engine journal bearing. This method calculates the friction force and the coefficient of friction by using the following equations:

$$F_s = \frac{e}{2R} F \sin\beta + B \frac{\eta}{\psi} r \omega \frac{2\pi}{\sqrt{1-\epsilon^2}} + 2\pi\eta BR \dot{\gamma} \cos 2\gamma \left[\frac{1}{\sqrt{1-\epsilon^2}} - 1 \right] \quad (6)$$

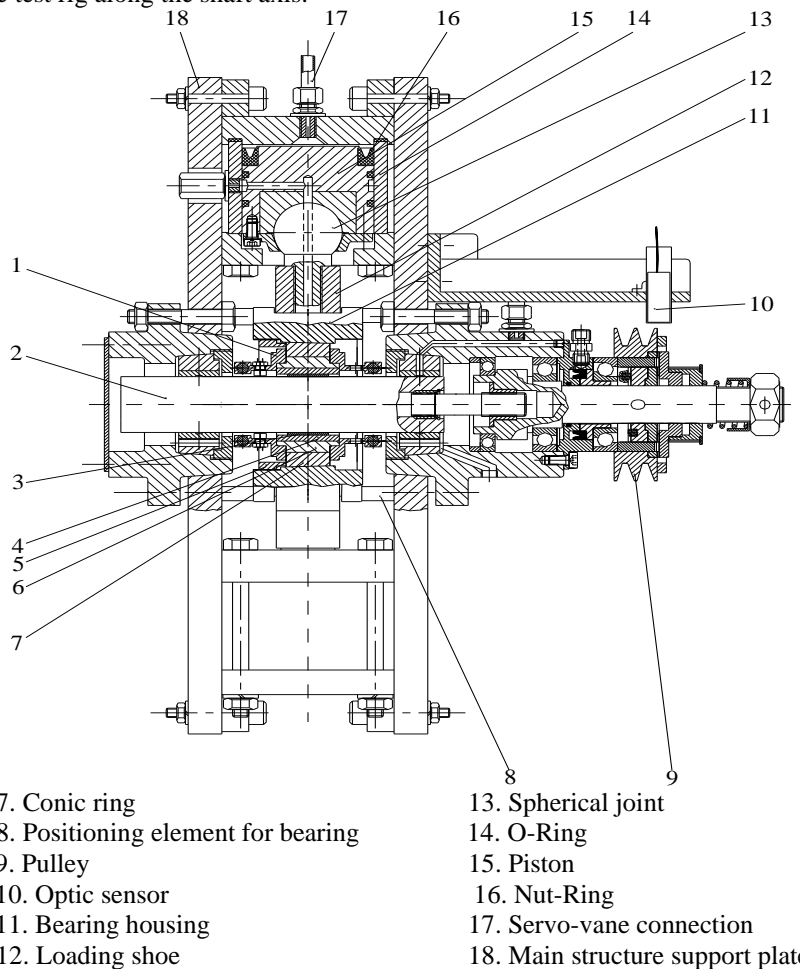
$$\mu = \frac{e}{2R} \sin\beta + \frac{B\eta r \omega}{F\psi} \frac{2\pi}{\sqrt{1-\epsilon^2}} + \frac{2\pi\eta BR}{F} \dot{\gamma} \cos 2\gamma \left[\frac{1}{\sqrt{1-\epsilon^2}} - 1 \right] \quad (7)$$

Bearing width	0.0265	m.
Bearing diameter	0.047750	m.
Radial clearance	0.030	mm.
Oil feed pressure	2×10^5	Pa
Oil viscosity	0.082	Pa.s
Shaft rotational speed	1240	rpm

3. EXPERIMENTAL BACKGROUND

3.1 Experimental setup

In this study, Karadeniz Technical University (KTU) laboratory test rig was utilized to investigate tribological behavior of the dynamically loaded engine journal bearing. The KTU laboratory test rig, which uses a direct method where the friction torque of only the test bearing is measured without any interference of the shaft-supporting bearings, was designed to measure friction force under dynamic loading conditions by Büyükioğlu [15] and then modified to measure the orbit of the journal center under dynamic load by Büyükioğlu et al. [16,18]. The description of the test rig is shortly presented in the following section although the detailed information about the test rig can be obtained from the above mentioned references and ref. [19]. Fig. 1 shows the cross-sectional views of the test rig along the shaft axis.



- | | | |
|-----------------|------------------------------------|----------------------------------|
| 1. Fixing ring | 7. Conic ring | 13. Spherical joint |
| 2. Journal | 8. Positioning element for bearing | 14. O-Ring |
| 3. Test bearing | 9. Pulley | 15. Piston |
| 4. Bearing cap | 10. Optic sensor | 16. Nut-Ring |
| 5. Screwed ring | 11. Bearing housing | 17. Servo-vane connection |
| 6. Bushing | 12. Loading shoe | 18. Main structure support plate |

Figure 1. Cross-sectional view of the test rig along journal axis[16].

The mainframe of the test rig consists of two main structural support plates along which four hydraulic loading cylinders mounted in between. These cylinders are positioned around the test bearing housing in 90° intervals forming two pairs, one pair on the vertical axis and the other on the horizontal axis. In each cylinder there is a piston made of the same material as the cylinder to prevent contraction due to different thermal expansion between piston and cylinder. The physical contact between the bearing housing and each cylinder is provided by a loading shoe, which is connected to the piston through a spherical joint which transmits the applied load continuously in the radial direction through sliding on its housing. The journal is made of AISI 1070 hardened steel with Rockwell C hardness of 55 and supported at each end by bronze support bearings with a radial clearance of 0.025 mm. The power taken from 5.5 kW motor with 1240 rpm is transmitted to the driven shaft by using a belt-pulley system and it reaches to the journal by using a geared shaft. The geared shaft also functions as a stabilizing element for misalignment along the bearing axes. The test rig consists of the hydraulic system and the lubrication unit in which the same types of oils were used. The hydraulic unit has a tank with 90 liters capacity, electrical motor, geared pump, pressure relief valve, and manometer while the lubrication unit consists of a tank having 40 liters capacity, geared pump driven by an electrical motor, filter, distribution room, pressure relief valve, heating element, manometers, and connection pipes.

3.2 Determination of frictional properties

The new measurement system constructed specially to measure friction force is schematically shown in Figure 2. When the journal is driven, the journal bearings housing also turned in the same direction as the journal due to the friction between the test bearing and the rotating journal. The frictional moment occurring between the journal bearings and bearing cap was measured by using a Wheatstone bridge circuit via the strain gauges. The conversion to a bending force was executed on the four measurement beams on which strain gauges attached to both sides give a signal proportional to the frictional moment. Two of these measurement beams are at the front end, while the others are at the rear end of the test bearing. A full-bridge circuit was set up by using four strain gauges. The signal taken from the bridge circuit was amplified with a KWS/T-5 model amplification and sent to a computer via a data acquisition system. The oscilloscope was included into the system to indicate the time history of net load along each axis passing through two opposing pairs of cylinders. The system was also capable of indicating the polar load diagram directly when all the connections were made onto one oscilloscope.

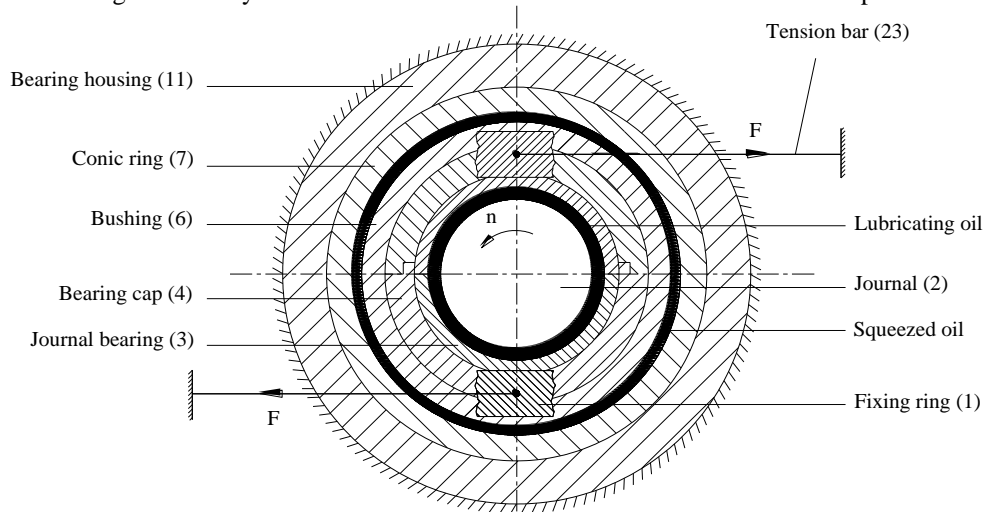


Figure 2. Schematic representation of the developed friction force measurement system[17].

The polar loads, two bearing load components (vertical and horizontal), and friction forces were then recorded by a DSO 400 GOULD model oscilloscope. An optic sensor was used to measure the crank angle during the experiments while four transducers were utilized to measure the journal center trajectory. Journal load, friction forces, and displacement of journal centre were measured from the record by every 15° crank angle intervals. The signal values were then converted into friction torque and friction force values, which were determined using a calibration line obtained from the strain gauges.

3.3 Test specimen and procedure

The bearings of S844-GS5049 M series used in the experiments were supplied by Sahin Engine Metal Company, Turkey. The geometry and the dimensions of the bearings are shown in Figure 3 while Figure 4 shows the photographs of plain, circumferential, herringbone, and transversally grooved journal bearings.

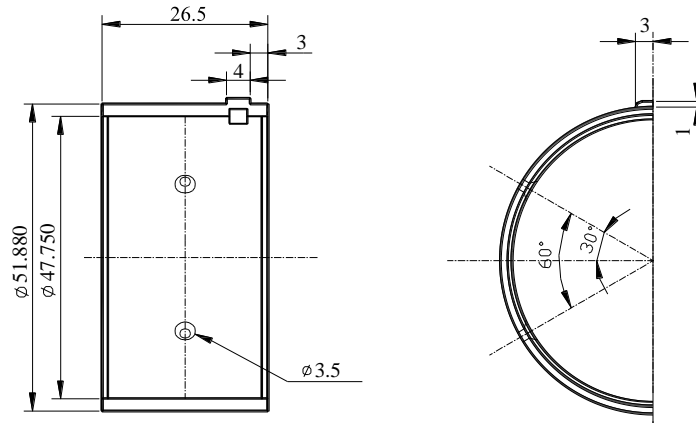


Figure 3. The shapes and dimensions of the test bearings

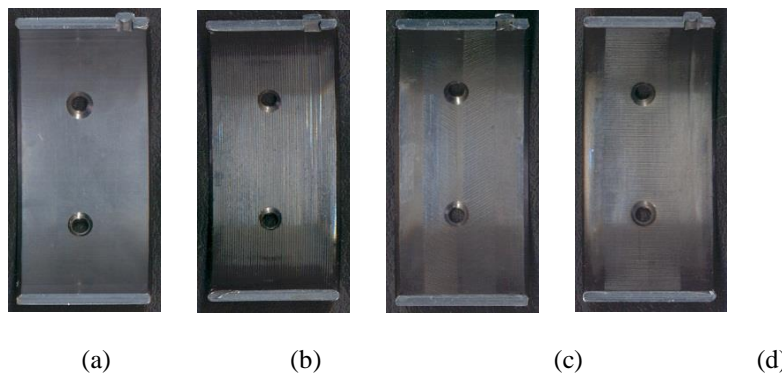


Figure 4. Plain (a) circumferentially (b) V-shaped (herringbone) (c) and transversally grooved (d) journal bearings

The circumferential, transverse and herringbone grooves were fabricated onto the plain engine bearing. The circumferential grooves were made with a hard 60° angle thread cutting tool tip whereas the transverse and the herringbone grooves were made by a 20x8x6 mm single wheel knurling tool used for general non-cutting forming purposes made by Zeus Company. Both grooves, transverse and the herringbone, made onto the plain engine bearing by pinching straight and 45° inclined grooves via knurling wheel made of HSS steel having a hardness of 62±1HRC, respectively. The surface profiles of the journal bearings measured prior and after the tests by using Perthometer M1, surface roughness measuring device. The average depths of all micro grooves are taken as 30 µm in this study. The journal bearing with circumferential grooves, the average roughness height before the tests is found to be 7.815 µm while the average roughness depth is 29.7 µm. On the other hand, however, the average roughness height (Ra) value of the presumably plain and smooth journal bearing is 1.040 µm while the average roughness depth is 4.86 µm [20].

Before starting the experiments, the calibration curve was obtained. Then, the test bearings were run for 2 h in order to flush out wear debris during the running-in process under low speed and low loading conditions. In order to provide temperature stability, the system was run for about 30 min. and the lubricant temperature reached 23°C. The experiments were carried out with commercial base oil [25].

4. RESULTS AND DISCUSSION

In order for only the lower part of the bearing to be under the effects of load, the load specimen's polar views taken from an oscilloscope screen and the applied load's horizontal and vertical components are given in Figure 5. The loads on the horizontal and vertical axes are completely variable and act on the bearing in a sinusoidal form of loading.

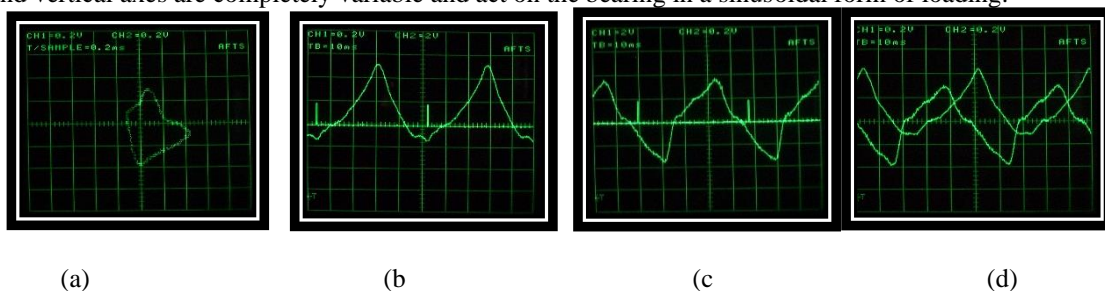


Figure 5. Polar load (a) horizontal (b) and vertical (c) loads components

In Figure 6, variations of horizontal and vertical components of dynamic load with their resultant are given with respect to bearing's crank angle. When the load specimen is investigated, it is found that the maximum bearing load is at 202.5 degree crank angle and 8520.94 N load value whereas the minimum bearing load is found at 315 degrees crank angle and 1483.64 N load value.

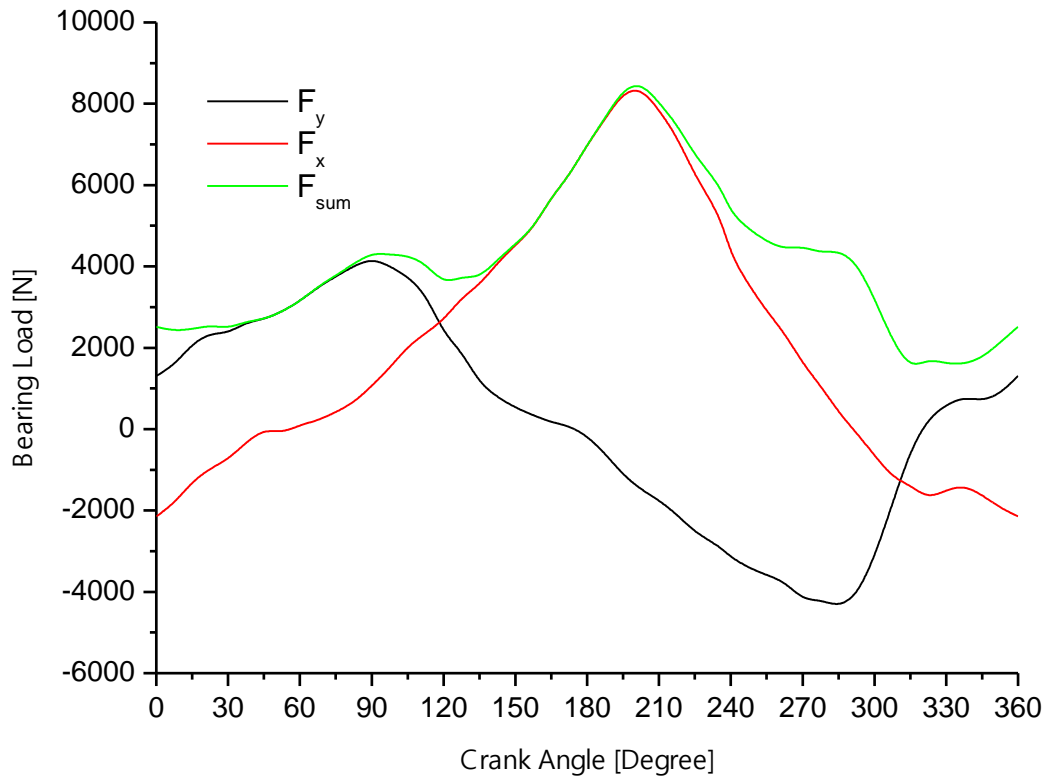


Figure 6. Variation of the vertical and horizontal loads as a function of crank angle

Variations of measured frictional forces formed on oil film on bearings with transversal, V-shaped and circumferential micro grooves as well as on non-grooved (plain) bearings under dynamic load are given in Figure 7. The frictional behaviors for the four different bearings under the same dynamic load are given collectively in Figure 10.

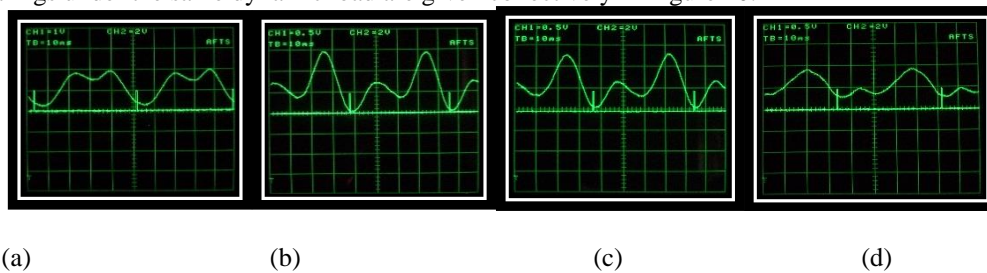


Figure 7. Variations of measured frictional forces formed on oil film on bearings with transversally, V-shaped and circumferentially and non-grooved (plain) bearings

Investigation of the measured frictional force distribution patterns shows that the lowest force of friction is exhibited on the plain journal bearing. From there, the force follows an increasing trend to circumferentially grooved, herringbone grooved and finally the highest frictional force is found at the transversally grooved journal bearing.

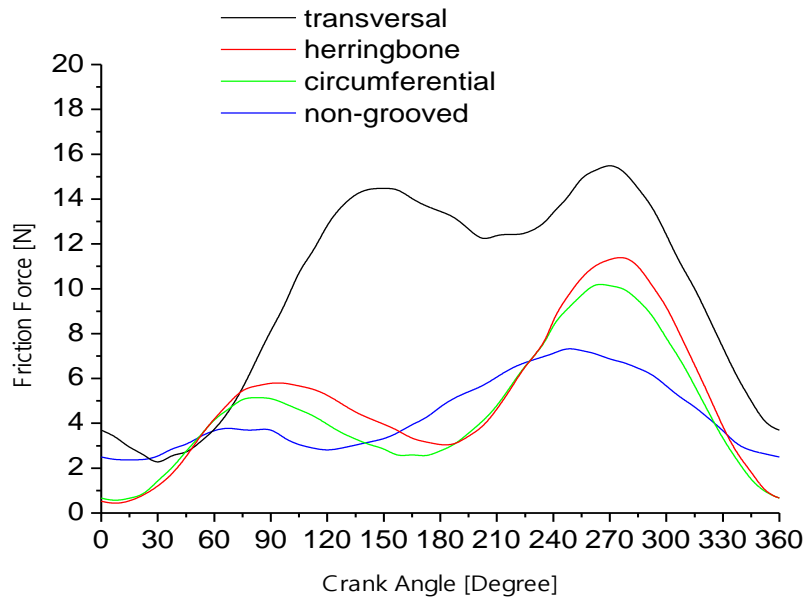


Figure 8. The frictional behaviors for the four different bearings under the same dynamic load

Observing Figure 8, it is found that the highest force of friction is 15.58 N and found at 270° crank angle on the transversally grooved bearing, followed, respectively, by 11.47 N at 277.5° crank angle on herringbone grooved bearing, 10.28 N at 262.5° crank angle on circumferential grooved bearing and 7.38 N at 247.5° crank angle on plain bearing. If these values are taken into consideration, the increasing ratios with respect to plain bearing are 2.11 times for transversally grooved bearing, 1.55 times for herringbone grooved bearing and 1.39 times for the circumferentially grooved bearing respectively.

The reason for the high frictional values on transversally grooved bearing can be described as the fact that during circumferential movement of the fluid, the fluid flow along the transversal channels is disrupted more than in the other types of grooves.

Coefficients of friction with respect to crank angles for the four types of bearings under the effects of specimen load are shown in Figure 9.

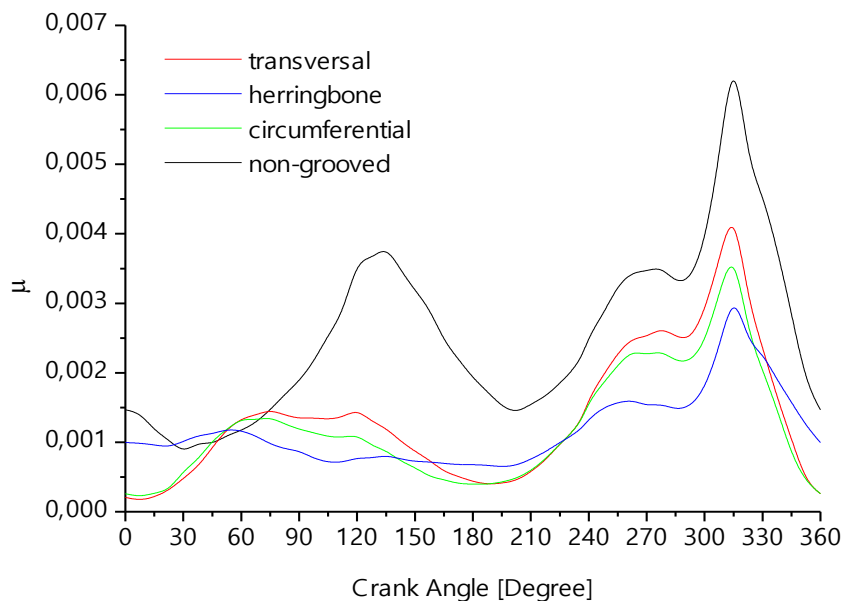


Figure 9. The friction coefficient for the four different bearings under the same dynamic load

When this Figure is studied, it is seen that the smallest value of coefficient of friction is exhibited on plain bearing while the largest is on transversally grooved journal bearing.

The maximum values of coefficient of friction obtained through measurements from the load specimen are 0.0067, 0.0044, 0.0038 and 0.0032 for transversal grooved, herringbone grooved, circumferential grooved and plain bearings respectively. The study of the values indicates that all the tests on all the bearings took place within the liquid friction zone.

The increasing ratios in coefficients of friction based on plain bearing are 2.09 times for transversally grooved bearing, 1.31 times for the herringbone grooved bearing and 1.18 times for the circumferential grooved bearing. The transverse channels on the transversally grooved bearings are the ones that led the said type of bearing to have higher value of coefficient of friction than the other types.

The graphs showing results of variation of frictional forces of bearing under load obtained by using Ricardo packet program, Mobility and Finite Difference Method, Schaffrath Method and from experimental analysis are shown in Figure 10.

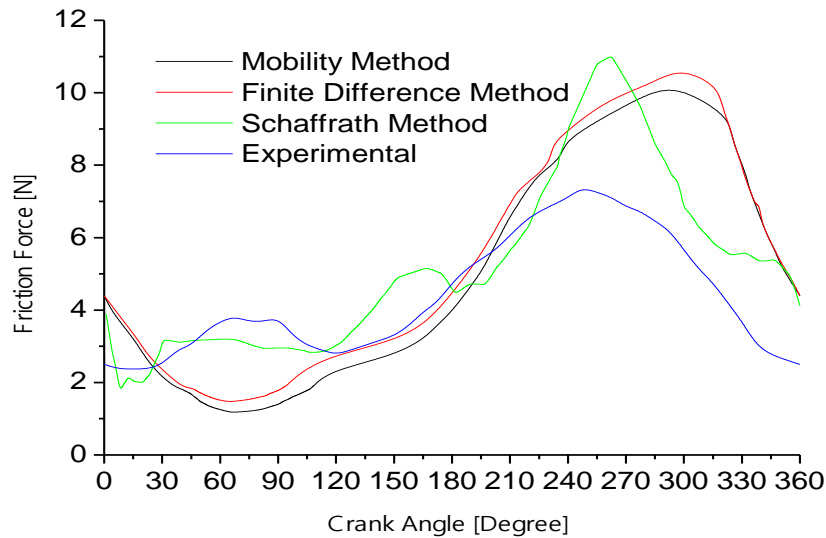


Figure 10. The variation of frictional forces of under bearing load obtained numerical and experimental analysis

When this figure is studied, it is seen that the highest frictional force on the mobility method is a value of 10.26N at 295° crank angle, while the highest frictional force on the finite difference method is 10.68 N at 298° crank angle and finally the values of friction force obtained with the Schaffrath method at 261° crank angle is 10.96 N and that obtained experimentally is 7.38N at 247.5° crank angle.

In Figure 11, variations of measured and calculated coefficients of friction on plain bearing specimen under the effects of load are shown.

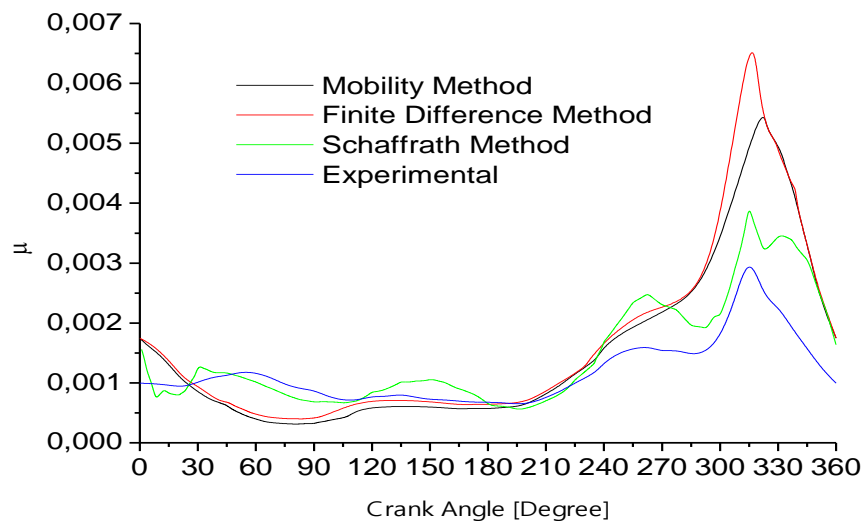


Figure 11. The variation of friction coefficient of under bearing load obtained numerical and experimental analysis

When the coefficients of friction obtained experimentally are compared with those obtained through measurements and calculation, it is found that their values are very close to each other and that the maximum value of coefficient of friction occurs almost at the same point. The orbits and polar load diagram drawn by the shaft center based on different computation methods on a radial journal bearing which is under the effects of loads are shown in Figure 12.

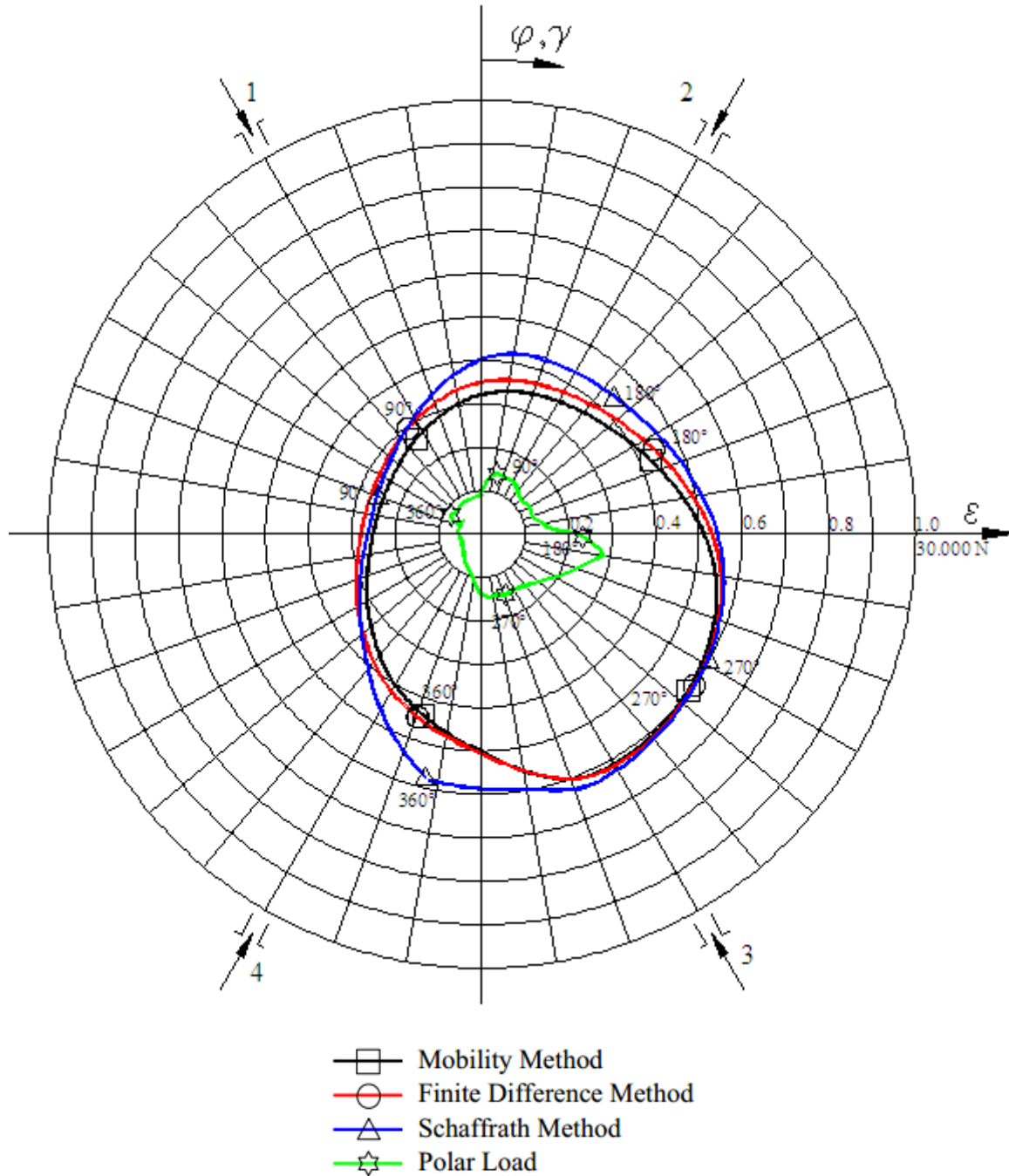


Figure 12. Polar load and journal center orbits

The figure shows that the orbits drawn by the shaft center comply well with each other and that any difference might be caused by the computation method used. It is also seen from the figure that the angle at which the maximum eccentricity ratio exist for all the three methods is approximately 155° with a value of 0.6. The graph plotted in order to determine the relationship between the experimentally obtained coefficients of friction on plain bearing and the minimum oil film thickness obtained from different numerical methods is given in Figure 13.

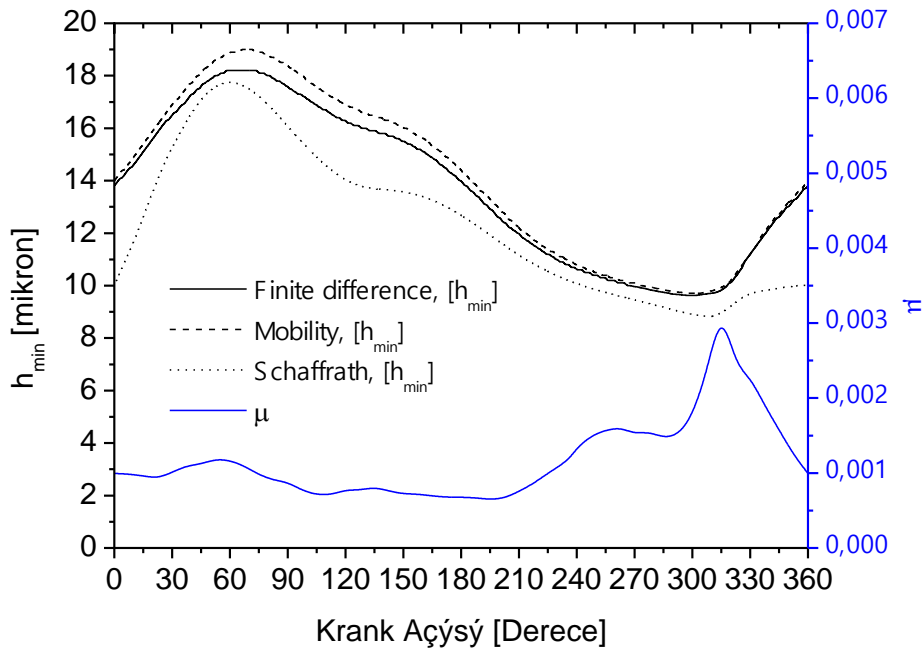


Figure 13. Coefficients of friction on plain bearing and the minimum oil film thickness obtained from different numerical methods

The figure shows that when the oil film decreases the coefficients of friction increase; and that the maximum value of coefficient of friction is obtained at a crank angle where the oil film thickness is minimum. Figure 14 shows the variation of minimum oil film thicknesses with respect to crank and position angles.

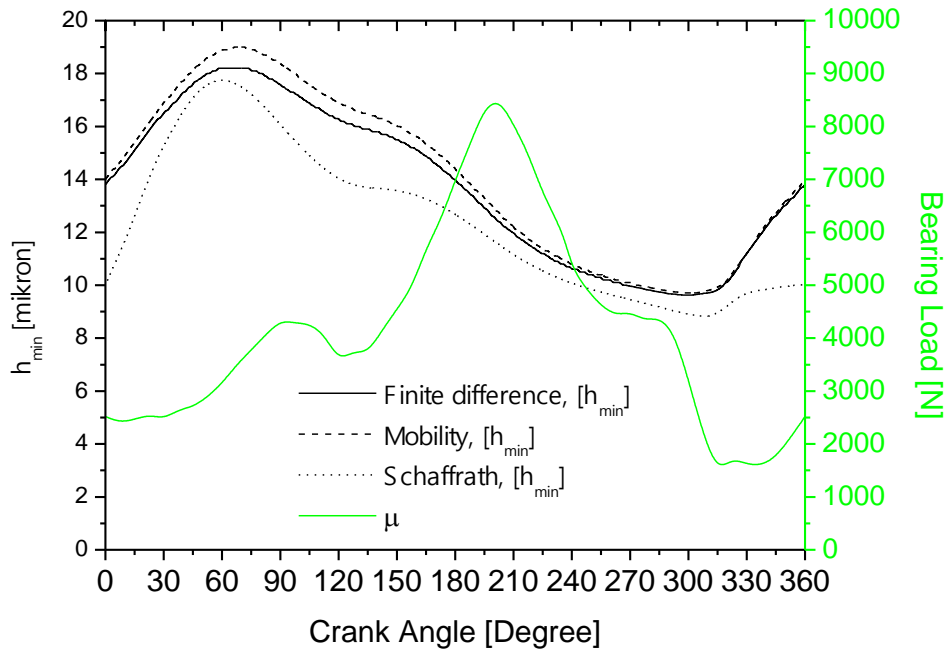


Figure 14. The variation of minimum oil film thicknesses with respect to crank and position angles.

The figure shows that the smallest oil film thickness is at an angle of around 155°. Due to the fact that the load reaches its maximum value at about 202.5°, then the position of minimum oil film thickness is at about 45° ahead of the maximum bearing load.

In Figure 15 variation of minimum oil film thickness with respect to bearing load is shown.

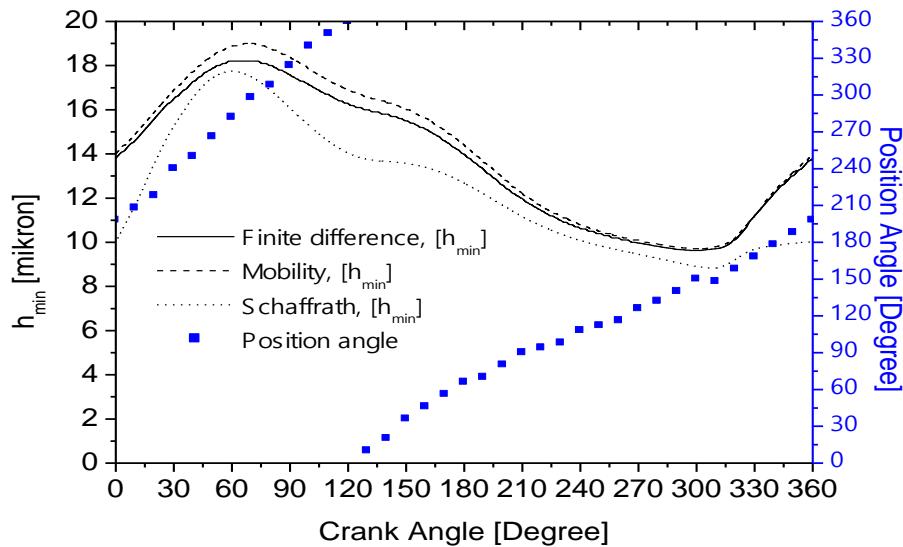


Figure 15. The variation of minimum oil film thickness with respect to bearing load

Investigation of the figure shows that with the mobility method the minimum oil film thickness is $9.71 \mu\text{m}$ and exists at $\Phi=298^\circ$ crank angle. The solution with the Finite Difference Method indicates the minimum oil film to be $9.63 \mu\text{m}$ and at the direction of $\Phi=298^\circ$, approximately the same crank angle. Whereas Schaffrath Method gave the minimum oil film thickness value of $8.82 \mu\text{m}$ at $\Phi=309.5^\circ$. A thorough study of the figure, moreover, shows that the minimum value of the oil film thickness is exhibited at a crank angle of 96° after passing the maximum value of load.

Surface profiles measured on a circumferential grooved radial journal bearing prior to and after the tests by using Perthometer M1 surface roughness measuring device are shown in Figure 18.

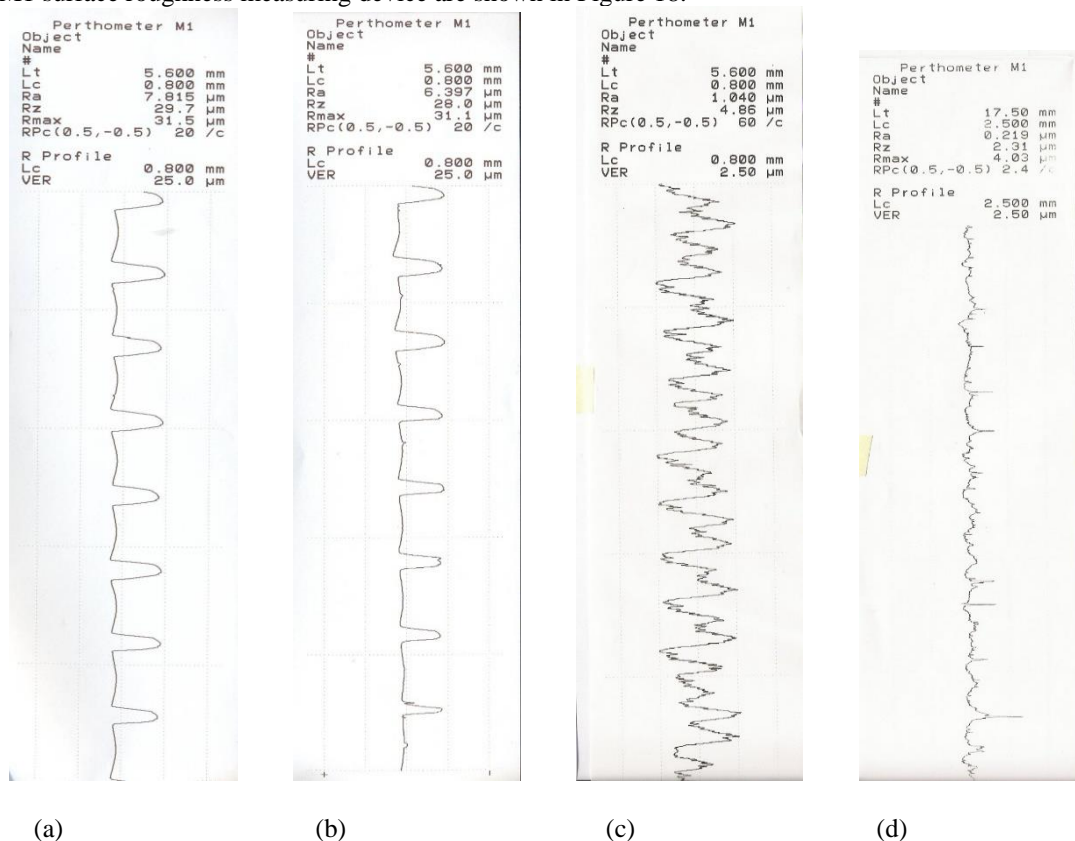


Figure 16 Surface profiles measured on a circumferential grooved bearing prior (a) to and after (b) the tests, plain journal bearing and test shaft

Whereas the journal bearing we assumed to be plain and the test device's surface profiles are given in Figure 16. When the profiles are investigated, it is interestingly, found that even the presumably plain and smooth engine bearing has some indents and protrusions; and that the average roughness height (Ra) value is 1.040 μm while the average roughness depth is 4.86. On the engine bearing with circumferential grooves, the average roughness height before the tests is found to be 7.815 μm while the average roughness depth is 29.7 μm . Here the purpose is compare the plain bearing (we assume to be smooth, although in reality it is not) that has deeper roughness with the engine bearing by cutting circumferential grooves on it and also to show how accuracy is our measurement system. This is so because during the tests it was observed that there was no metal to metal contact between the components as there was an oil film in between them. If there were a metal to metal contact, the coefficients of friction would increase abruptly. In fact it is quite clear that friction on the other groove forms, herringbone and transversal grooves, would be higher, however, the test results of these bearings are also given here in order to make comparisons. It is also, investigated, in this study to see which type of bearing groove exhibits higher friction. This is important information for researchers dealing with engine bearings and for industrialists too.

As it was explained on the literature abstract that in recent years there have been ongoing researches on microgrooved engine bearings in Japan. There are studies in literature showing that in circumferential grooved bearings the friction and hence wear is exhibited is small at the start of motion due to the fact that always some lubricants remain in these types of grooves.

In our study, we investigated the effects of micro grooves on frictional behavior within liquid friction zone. Because the grooves we used in the tests were relatively large, we could not see the results that the friction decreases on the circumferentially grooved bearings but the bearing we assumed that it is plain was just like the circumferential grooved bearing. The average roughness values of the so assumed smooth bearing were relatively smaller than those of the circumferentially grooved bearings.

5. CONCLUSIONS

With the developed frictional force measuring system, grooves in micron scale basis in circumferential, transversal and herringbone forms were opened onto plain bearings and then the microgrooved bearings were subjected to static and dynamic load where their behaviors were investigated numerically and experimentally. This investigation yielded the following:

1. When variations of frictional forces on the oil film for different types of bearings (transversally, circumferentially, herringbone grooved bearings and the plain bearing,) under same dynamic loading conditions are studied, it is seen that the lowest value of frictional force is found on the plain journal bearing. Then the values progressively increase on the circumferential grooved bearing, herringbone grooved bearing and the highest frictional force distribution is at the transversal grooved bearing. The reason for the higher frictional force value on the transversally grooved bearing can be said to be a higher disruption of the oil flow in this type of bearing by the grooves as compared to the other forms of grooves during circumferential motion of the fluid.
2. It is found that the values of coefficients of friction specified under dynamic load take the lowest value on plain and non grooved bearing whereas on the value becomes maximum on transversally grooved bearings.
3. The average increases in frictional forces based on a plain surface journal bearing are approximately 1.39 times on a circumferentially grooved bearing, 1.55 times on a herringbone grooved bearing and 2.11 times on a transversally grooved bearing.
4. The average increases in coefficients of friction based on a plain surface journal bearing are approximately 1.18 times on a circumferentially grooved bearing, 1.31 times on a herringbone grooved bearing and 2.09 times on a transversally grooved bearing.
5. When the graphs of frictional force behaviors obtained with different solution methods and those obtained with numerical methods are compared with those obtained by measurements on plain surface journal bearing, it is seen that their curves are very similar and comply well with each other.
6. It is also found that the values of coefficients obtained numerically and those obtained experimentally are very close to each other.
7. Comparison of orbits drawn by shaft center based on different computation methods, shows that the orbits are very close to each other.
8. Investigation of the graphs of minimum oil film thickness with respect to crank angle and position angle indicates that the lowest oil film thickness value is exhibited at a farther position past the point of maximum load value.
9. In variation of minimum oil film thickness on a bearing under dynamic load, it is found that the oil film decreases as the coefficients of friction increase throughout a loading period, and that when the oil film thickness reaches its minimum value, the coefficient of friction takes its maximum value.

In conclusion, the results of this research showed that the shape of micro groove plays an important role in the oil film thickness, the coefficient of friction, and friction force under the dynamic load. As mentioned above, the researchers have, without concerning any operating conditions, concluded that the micro-grooved journal bearings had very high resistance to seizure and fatigue, lower temperature of the bearings under high loading conditions and the minimum oil film thickness of micro-grooved bearings was thicker than that of the traditional plain bearings due to the oil being retained in the grooves. However, this study showed that although having micro grooves on the surface of journal bearings was proved to be an effective method to enhance the tribological behavior of the journal bearings under starved lubrication conditions (during

start-up and stopping movements) as recommended in the literature, there is a probability of developing the worse tribological properties when engine bearings operate in the liquid friction zone under different conditions such as regular operating range (in between start-up and stopping range) as shown in this study. This study further indicated that the use of generalized results regardless of type of micro groove and operating condition may result in erroneous estimates of the tribological properties of the micro-grooved journal bearing. It is, therefore, recommended that performing detailed investigation in conjunction with shape, depth and operating condition of the micro-grooved journal bearing is necessary to obtain reliable data regarding the tribological properties of the micro-grooved journal bearing.

6. REFERENCES

- [1] Hu J. Experimental and theoretical investigation of roughness effects on thin laminar fluids films. PhD thesis. University of Toronto, Canada; 1997.
- [2] Zhang C, Qiu Z. Effects of surface texture on hydrodynamic lubrication of dynamically loaded journal bearings. *Tribology Transactions STLE* 1998;41:43–8.
- [3] Christensen H, Tonder K. The hydrodynamic lubrication of rough bearing surfaces of finite width. *Journal of Lubrication Technology—Transactions of the ASME* 1971;93:324–330.
- [4] Christensen H, Tonder K. The hydrodynamic lubrication of rough journal bearings. *Journal of Lubrication Technology—Transactions of the ASME* 1973;95:166–72.
- [5] Hata H, Nakahara T, Aoki H. Measurement of friction in lightly load hydrodynamic sliders with striated roughness, The Winter Annual Meeting of the ASME, Chicago, Illinois, 75–92; 16–21 November 1980.
- [6] Nakahara T, Takesue M, Aoki H. Effects of surface roughness and bearing slenderness ratio on hydrodynamic lubrication. *Journal of JSLE* 1983;28:543–8.
- [7] Nakahara T. Effect of truncation in surface roughness on hydrodynamic pivoted slider and practical expression of truncation. In: Andersson P, Ronkainen H, Holmberg K, editors. 9th NORDTRIB, 3; 2000. p. 935–44.
- [8] Kumada Y, Hashizume K, Kimura Y. Performance of plain bearings with circumferential micro grooves. *Tribology Transactions STLE* 1996;39:81–6.
- [9] Hargreaves DJ, Armatsy D. Performance of a microgrooved journal bearing under steady and dynamic loading. *Tribo-Test* 1999;5:277–86.
- [10] Watanabe K, Natsuma J, Hashizuma K, Ozasa T, Noda T, Masuda Y. Theoretical analysis of bearing performance of microgrooved bearing. *JSAE Review* 2000;21:29–33.
- [11] Roy L. Thermo-hydrodynamic performance of grooved oil journal bearing *Tribology International* 2009;42:1187–98.
- [12] Hirayama T, Yamaguchi N, Sakai S, Hishida N, Matsuoka T, Yabe H. Optimization of groove dimensions in herringbone-grooved journal bearing for improved repeatable run-out characteristics. *Tribology International* 2009;42:675–81.
- [13] Ricardo Software, *Journal Bearing Analysis-Orbit, Documentation/User Manual Version 1.2, USA; 2000.*
- [14] Schaffrath G. The lubricating bearings with arbitrary gap shape-shifting of the shaft journal with time-varying load. PhD thesis. Technical University, Karlsruhe, Germany (in German); 1967.
- [15] Harbordt J, Klumpp R. Computer program for calculating the displacement train, the local pressures and the factual gap lubricating bearings in arbitrary geometry under static and dynamic load, Research Reports Internal Combustion Engine Projects, No. 98, Issue 137; 1972 (in German).
- [16] Biyikoglu A. Surface fatigue on dynamically loaded journal bearings. PhD thesis. Karadeniz Technical University, Trabzon, Turkey; 1986 (in Turkish).
- [17] Durak E, Kurbanoglu C, Biyikoglu A, Kaleli H. Measurement of friction force and effects of oil fortifier in engine journal bearings under dynamic loading conditions. *Tribology International* 2003;36:599–607.
- [18] Biyikoglu A, Cuvalci H, Adatepe H, Bas H, Duman MS. A new measurement test apparatus and method for the friction force measurement in the journal bearings under dynamic loading Part I. *Experimental Techniques* 2005;29:22–5.
- [19] Biyikoglu A, Cuvalci H, Adatepe H, Bas H, Duman MS. A new measurement test apparatus and method for the friction force measurement in the journal bearings under dynamic loading Part II. *Experimental Techniques* 2005;29:33–6.
- [20] Adatepe H. The investigation of the friction behavior of the microgrooved journal bearings under static and dynamic loading conditions. PhD thesis, Karadeniz Technical University, Trabzon, Turkey; 2006 (in Turkish).
- [21] Adatepe H, Biyikoglu A, Sofuoglu H. An experimental investigation on frictional behavior of statically loaded micro-grooved journal bearing. *Tribology International* 2011;44:942–8.
- [22] Booker JF. Dynamically loaded journal bearings: mobility method of solution. *Journal of Basic Engineering—Transactions of the ASME* 1965;4:537–46.
- [23] Booker JF. Dynamically loaded journal bearings: numerical application of mobility method. *Journal of Lubrication Technology—Transactions of the ASME* 1971;93:168–76.
- [24] Goenka PK. Analytical curve fits for solution parameters of dynamically loaded journal bearings. *Journal of Tribology—Transactions of the ASME* 1984;106:421–8.
- [25] Adatepe H, Biyikoglu A, Sofuoglu H. An investigation of tribological behaviors of dynamically loaded micro-grooved journal bearing. *Tribology International* 2013;58:12–19.